

1-25-12  
E-6761

NASA Technical Memorandum 105374  
AIAA-92-0647

# Results of an Icing Test on a NACA 0012 Airfoil in the NASA Lewis Icing Research Tunnel

Jaiwon Shin and Thomas H. Bond  
*Lewis Research Center*  
*Cleveland, Ohio*

Prepared for the  
30th Aerospace Sciences Meeting and Exhibit  
sponsored by the American Institute of Aeronautics and Astronautics  
Reno, Nevada, January 6-9, 1992



# Results of an Icing Test on a NACA 0012 Airfoil in the NASA Lewis Icing Research Tunnel

Jaiwon Shin<sup>†</sup> and Thomas H. Bond<sup>†</sup>

National Aeronautics and Space Administration  
Lewis Research Center  
Cleveland, Ohio 44135

## Abstract

Tests were conducted in the Icing Research Tunnel (IRT) at the NASA Lewis Research Center to document the current capability of the IRT, focused mainly on the repeatability of the ice shape over a range of icing conditions. Measurements of drag increase due to the ice accretion were also made to document the repeatability of drag. Surface temperatures of the model were obtained to show the effects of latent-heat release by the freezing droplets and heat transfer through the ice layer. The repeatability of the ice shape was very good at low temperatures, but only fair at near freezing temperatures. In general, drag data shows good repeatability.

## Introduction

Over the past few years, the Icing Research Tunnel (IRT) at the NASA Lewis Research Center (LeRC) has gone through several rehabilitations which have improved its capabilities in simulating real icing conditions. Some of the improvements include a new and more powerful fan motor, a new spray bar system, a new digital control system, and various improvements to the IRT structure. As a result, the IRT can now provide more accurate control of the airspeed and temperature, more uniform clouds covering a larger cross-section of the test section, and lower liquid water content.

Although various test programs have been conducted in the IRT with the improved capabilities, there has not been a comprehensive test program to document the repeatability of the data obtained in the IRT. With the increasing use of experimental data for code validation work, there is a need for a repeatability study of the experimental ice shape and drag.

Tests were conducted to address the repeatability issue in the IRT during the months of

June and July of 1991. The test matrix was focused to document the repeatability of the ice shape over a range of icing conditions including airspeed, air temperature, liquid water content (LWC), and spray time. During the tests, the drag increase due to the ice accretion and the surface temperature were also measured. In this paper, results from the test are presented.

## Nomenclature

$c$	airfoil chord
$C_d$	drag coefficient
$T_t$	total air temperature
$T_s$	model surface temperature
$V_\infty$	airspeed
$x$	surface coordinate
$y$	coordinate perpendicular to $x$

## Description of the Experiment

### Icing Research Tunnel

The NASA Lewis Icing Research Tunnel is a closed-loop refrigerated wind tunnel. Its test section is 6 ft. high, 9 ft. wide, and 20 ft. long. A 5000 hp fan provides airspeeds up to 300 mph in the test section. The 21,000-ton-capacity refrigeration system can control the total temperature from -40°F to 30°F. The spray nozzles provide droplet sizes from approximately 10 to 40  $\mu\text{m}$  median volume droplet diameters (MVD) with liquid water contents (LWC) ranging from 0.2 to 3.0 g/m<sup>3</sup>. A schematic of the tunnel, shop, and control room is shown in Fig.1. A detailed description of the IRT can be found in reference 1.

### Test Model

The test model was a 6 ft. span, 21 in. chord

---

<sup>†</sup>Aerospace Engineer

NACA 0012 airfoil with a fiberglass skin. The model was mounted vertically in the center of the test section. During all icing runs, the model was set at 4° of angle of attack. The model installed in the test section is shown in Fig.2.

Five type T thermocouples were installed underneath the fiberglass skin at the leading edge. Each thermocouple is 1 foot apart along the span as shown in Fig.3. Measurement accuracy of the thermocouple is specified to be  $\pm 0.9^{\circ}\text{F}$ .

### Test Conditions

Test points were selected to study the effects of air temperature, LWC, and spray time on the repeatability of the ice shape. Test conditions are listed in Table 1 and 2.

Table 1 lists the test points used to study the effect of air temperature on the repeatability of the ice shape. Temperatures were selected to cover glaze, rime, and transition regimes. The test conditions can be divided into two groups: 1) low airspeed and high LWC, and 2) high airspeed and low LWC. Water droplet size was held constant for both groups. Airspeed, LWC, and spray time were selected so that both groups would have the same water intercept (i.e.  $\text{airspeed} \times \text{LWC} \times \text{spray time} = \text{constant}$ ).

The low airspeed, high LWC conditions were run for both 6 and 12 minute ice accretion times to investigate the effect of spray time on the repeatability of the ice shape. Test conditions for both spray times are listed in Table 1.

A few tests were also performed with LWC varying from 1.0 to 1.8 g/m<sup>3</sup> to determine if LWC affected the repeatability of the ice shape. The conditions for these tests are shown in Table 2.

### Test Methods

A typical test procedure for icing runs is listed below.

1. The model angle of attack was set.
2. The target airspeed and total temperature were set.
3. The spray system was adjusted to the desired MVD and LWC.

4. The spray system was turned on for the desired spray time.
5. The tunnel was brought down to idle and the frost beyond the ice accretion was removed.
6. The wake survey was traversed across the airfoil wake with the tunnel at the target airspeed.
7. The tunnel was brought down to idle again for ice shape tracings and photographs.
8. The airfoil was then cleaned and the tunnel conditions set for the next data point.

To record the ice shape, a heated metal template was used to melt the ice, and the shape was manually traced onto a cardboard template. Ice shape tracings were made at three spanwise locations for each icing run.

### Drag Wake Survey

The section drag at the mid-span of the airfoil was calculated from total pressure profiles measured by a pitot-static wake survey probe. The method for reducing the data is described in reference 2. The wake survey probe was positioned two chord lengths downstream of the airfoil as shown in Fig.2. The wake surveys were made only when the spray cloud was turned off. During sprays, the probe was kept behind a shield to prevent any ice accretion on the tip of the probe. The wake probe was mounted on an automatic traverse system, and the traversing speed was adjustable.

The data from the wake survey was stored by the Escort system which was developed at the NASA LeRC for storing, analyzing experimental data from various facilities at the center. A separate program was used to further analyze the wake data to get wake profiles and drag coefficient.

### Results and Discussion

This section contains a discussion of the quality of the airfoil drag data, and discussions of the test results including the repeatability of the ice shape, resulting drag, and the surface temperature data.

#### Quality of Experimental Drag Data

Dry airfoil drag results - Section drag was measured with the clean airfoil under the dry condition and the results are compared with the published data of references 3, 4, and 5 as shown



in Fig.4. The data of Abbott and Doenhoff<sup>4</sup> was taken in the Low Turbulence Pressure Tunnel (LTPT) at the NASA Langley Research Center. The data of Olsen, et al.<sup>3</sup> and the data of Blaha and Evanich<sup>5</sup> were taken in the IRT.

The LTPT data can be considered as an ideal baseline because the data was obtained in the tunnel with a very low freestream turbulence intensity (something of the order of a few hundredths of 1 percent) and the surface of the model was prepared with extreme care. The freestream turbulence intensity in the IRT (about 0.5 percent) is higher than that of the LTPT. Since models used in the IRT were for icing tests, the kind of surface finish used in the LTPT was not required. For these reasons, airfoil drag measured in the IRT could give a little higher drag coefficients than the LTPT data as shown in Fig.4 except Olsen's data which showed good agreement with the LTPT data.

The current IRT drag data is higher than the previous IRT data. All three tests used the wake survey method and the airfoils had the same chord length. This kind of difference in drag data can come from differences in the test itself and model condition. The leading edge and the trailing edge part of the current model were joined at the maximum thickness location (30 percent of the chord) while the model used in both reference 3 and 5 was the same one-piece airfoil.

According to the experimental results of Gregory and O'Reilly<sup>6</sup> shown in Fig.5, transition occurs at around 40 percent chord at 0° of angle of attack for an NACA 0012 airfoil at a Reynolds number of 3 million. The transition location moves upstream very rapidly as the angle of attack increases. A small step at the joint in the current model may have acted as a trip at low angles of attack causing an early transition to turbulent boundary layer. At higher angles of attack, the step may have acted as an additional roughness source in the turbulent boundary layer, which increased drag.

Drag associated with an iced airfoil is normally dominated by the pressure drag due to a large separation caused by a pressure spike at the upper horn. At 4° of angle of attack, where all the icing runs were made, an increase of the friction drag by

the step of the current model is believed to have a minimal effect on icing drag data.

#### Repeatability of dry airfoil drag measurements

- Dry runs were made prior to each icing run. Twenty-eight dry airfoil drag measurements were sampled at a 4° angle of attack. The percent variation of the measured drag coefficient was calculated in the same way as Olsen<sup>3</sup> by taking the standard deviation and dividing it by the average. The average Cd value at a 4° angle of attack was 0.01068. The percent variation was  $\pm 7.1$  percent of the average value. The percent variation reported by Olsen was  $\pm 7.7$  percent.

#### Experimental Repeatability of Ice Shape and Drag

Effect of air temperature - The effect of air temperature on the repeatability of the ice shape and drag was studied over a range of air temperatures covering from glaze to rime ice. Results are presented here only for typical glaze, rime, and transition ice. The airspeed was set at 150 mph and the accretion time was 6 minutes. The resulting ice shape showed typical glaze ice accretion with the characteristic upper ice horn at the total air temperatures of 28, 25, and 22°F. At -15°F, the ice shape was that of typical rime ice. The ice accretion at 12°F displayed a transition shape.

Figure 6 shows ice shapes traced at the mid-span and corresponding drag coefficients for the low-air-speed, high-LWC case (150 mph, 1.0 g/m<sup>3</sup>). At each temperature, ice shape tracings from all repeat runs are overlaid. The repeatability of the ice shape is fairly good at 28°F (Fig.6 a), 25°F (Fig.6 b), and 22°F (Fig.6 c), except the third run at 25°F, where thicker ice is seen. Ice horn growth and the thickness of ice repeat well at all three temperatures. Icing limits at the upper and the lower surface show good repeatability. The repeatability of the ice shape was best at the lowest temperature, -15°F (Fig.6 e). Overall repeatability of the drag coefficient was typically within the experimental variation for a clean airfoil.

Figure 7 presents data for the high-air-speed, low-LWC case. For these tests, the airspeed was 230 mph and the LWC was 0.55 g/m<sup>3</sup>. These values give the same water intercept as the 150-mph, 1.0-g/m<sup>3</sup> case of Fig.6. Water droplet size

was again kept constant at 20  $\mu\text{m}$ . The resulting ice shape is that of glaze ice at 28°F (Fig.7 a), 25°F (Fig.7 b), and 22°F (Fig.7 c), even though the upper horn is not as dominant as for the 150-mph, 1.0-g/m<sup>3</sup> case. The ice shape at 12°F (Fig.7 d) is more of that of rime ice, and the ice shape is that of typical rime ice at -15°F (Fig.7 e). As seen for the 150-mph, 1.0-g/m<sup>3</sup> case, the repeatability of the ice shape is fair at 28, 22, and 12°F, and very good at -15°F. The repeatability of the ice shape at 25°F is not as good as that with other temperatures. The variation of the drag coefficient is comparable with that of the 150-mph, 1.0-g/m<sup>3</sup> case.

Standard nozzles were used for the 150-mph, 1.0-g/m<sup>3</sup> case whereas mod-1 nozzles were used for the 230-mph, 0.55-g/m<sup>3</sup> case. Both sets of nozzles show similar repeatability of the ice shape for the temperature range tested.

Effect of spray time - The effect of spray time on the repeatability of the ice shape was studied by extending the spray time to 12 minutes for the 150-mph, 1.0-g/m<sup>3</sup> case. Since the repeatability of rime ice was shown to be very good, only the glaze ice conditions were tested. Figure 8 shows good repeatability in the ice shape at 28°F (Fig.8 a) and 22°F (Fig.8 c). As with the 6-minute-spray tests, the repeatability at 25°F (Fig.8 b) is not as good as that with the other temperatures. The repeatability of drag coefficient is fairly good for all three temperatures.

Effect of LWC - The effect of LWC on the repeatability of the ice shape and drag is shown in Fig.9. LWC used for this part of the test was fairly high, ranging from 1.0 to 1.8 g/m<sup>3</sup>. The spray time was 6 minutes which resulted in fairly large accretions of ice for all conditions. The total air temperature was set at 22°F which produced typical glaze ice. The airspeed was 230 mph and the MVD was 30  $\mu\text{m}$ .

Figure 9 (a) gives results for 1.0 g/m<sup>3</sup>, 9 (b) for 1.3 g/m<sup>3</sup>, 9 (c) for 1.6 g/m<sup>3</sup>, and 9 (d) for 1.8 g/m<sup>3</sup>. The ice shapes from the first and the second runs were not aligned for any of the four LWCs. Although the ice shapes show a shift between two runs at each condition, the ice shapes look very

similar. Drag data also shows good repeatability; this suggests that the ice shapes did in fact repeat well. The shift was probably caused by the fact that all the first runs were traced by one person and all the second runs were traced by another person.

The recorded ice shape could vary depending on a data taker because of differences in personal preferences in making a tracing. However these human elements only affect small details in the ice shape and do not normally affect the overall ice shape. More important factor for a possible discrepancy in a recorded ice shape is how a person uses a pencil while tracing the ice shape. The ideal way to trace the ice shape is to have a pencil stand perpendicular to a cardboard template. If the angle at which the pencil contacts the template is different between data takers, a shift such as seen in Fig.9 can happen.

An exercise was performed to document the magnitude of the variation in the ice shape due to the human elements involved during ice shape tracings. An ice shape at the mid-span from one icing run was traced by three individuals; the resulting shapes are shown in Fig. 10. Some of the details in the ice shape varied with data takers, and a minor shift was also seen. However, overall ice shapes agreed well and the magnitude of the variation in the ice shape was within the experimental repeatability. This kind of agreement is typical and the variation seen in the LWC-effect case does not normally occur.

Effect of spray nozzle - Some conditions in the IRT operating envelope can be obtained by either standard or mod-1 nozzles as shown in Fig.11. Ice shapes for the LWC=1.0 case were obtained using both nozzles to study whether a common icing condition could be effectively duplicated by either set of nozzles. Figure 12 shows the result, and the ice shapes show good agreement. The variance in drag coefficient was no greater than typically seen for other repeat tests reported here and only slightly higher than variation in typical dry-airfoil drag coefficients.

#### Effect of Cloud Uniformity on Spanwise Variation in Ice Shape

The IRT has been calibrated and the uniformity of the spray cloud has been documented<sup>7</sup>. Contour maps of the LWC in the test

section are shown in Fig.13 (Ref.7) for the standard and mod-1 nozzles. The area of uniform cloud obtained using the mod-1 nozzles is smaller than that using the standard nozzles. In order to document spanwise variation in the ice accretion within the uniform spray cloud, multiple tracings along the span were taken with each icing run .

Figure 14 shows the spanwise variation of the ice shape with the standard nozzles. Figure 14 (a) is for a temperature of 28°F, 14 (b) for 12°F, and 14 (c) for -15°F, covering glaze, transition, and rime ice. Ice shape tracings were taken at the three spanwise locations, 18, 36, and 54 inches, measured from the tunnel ceiling. 18 and 54 inches represent the top and bottom boundaries of the uniform test section cloud for the IRT standard nozzles shown in Fig.13 (a). The results show close agreement in the ice shape between the 36 and 54 inch locations, and with slightly less ice accreted at the 18 inch location. This result is consistent with the LWC distribution shown in Fig.13 (a), where the LWC varies little from the lower boundary of the uniform cloud to the center but begins to decrease near the top.

Figure 15 shows the ice shapes with the mod-1 nozzles at three spanwise locations: 24, 36, and 48 inches. The top and bottom locations represent the boundaries of the uniform test section cloud shown in Fig.13 (b). Results for temperatures of 28°F (Fig.15 a), 12°F (Fig.15 b), and -15°F (Fig.15 c) are shown. At all three temperatures, the thickest ice is seen at the mid-span (36 inches). At the top and bottom locations, the ice accretion is very similar in both mass and shape. This result is again consistent with the LWC distribution shown in Fig.13 (b), where the LWC is approximately equal at the top and bottom of the uniform test section cloud map.

In order to validate the observations made above, the repeatability of the ice shape at the top and the bottom spanwise locations was also investigated. Figure 16 shows the comparison of the ice shape from repeat runs at the top location with the airspeed of 150 mph. The repeatability is good at 28°F (Fig.16 a) and 12°F (Fig.16 b). At -15°F (Fig.16 c), good agreement was shown between the third and the fourth runs, but agreement was not so good with the other two runs.

The repeatability of the ice shape at the bottom location with the airspeed of 150 mph is shown in Fig.17. The repeatability is good at all temperatures. The repeatability of the ice shape at the top and bottom locations for 230 mph is not shown here, but the results showed good repeatability at all temperatures. Generally, the repeatability of the ice shape at top and bottom locations was as good as the repeatability at the mid-span. However, in some cases, the quantity of ice accreted decreased with the distance from the center of the tunnel. Based on these observations, it is recommended that ice shape tracings be made at the mid-span for any data purpose.

#### Model Surface Temperature

Surface temperatures were monitored at several locations of the model as shown in Fig.3. Some of the results of the temperature data from the thermocouples located at the leading edge along the model centerline are reported in this section.

Heat transfer to model surface - The surface temperature during the ice accretion process was monitored at the mid-span leading edge. Time histories of the surface temperature are shown in Fig.18 at five tunnel air temperatures: 25, 22, 12, 1, and -15°F. The results show that the surface temperature before the spray began was very close to the tunnel air temperature. It normally took 10 to 15 seconds for spray cloud to reach the model in the test section. Once the ice accretion started, the surface temperature increased due to the release of the latent heat of freezing. This temperature rise was as large as 17 degrees for an air temperature of -15°F. As the accretion time elapse increased, the insulating ice became thicker, and, as a consequence, the heat transfer from the freezing droplets to the model surface decreased. This is seen by the decrease in the surface temperature with time. The repeatability of the surface temperature data was good as shown in Fig.19. The variation was less than 1°F which is within the uncertainty of the measurement.

Spanwise variation - Spanwise variation of the model surface temperature was examined at various tunnel air temperatures with airspeeds of 150 and 230 mph. The thermocouples were located at every foot from the top of the model as shown in Fig.3. Comparisons among the surface temperatures at the

leading edge were made in two groups: 1) at 2, 3, and 4 ft. along the span and 2) at 1, 3, and 5 ft. along the span. Only the results at  $-15^{\circ}\text{F}$  with an airspeed of 150 mph are presented here in Fig.20. Temperature profiles look very similar at all spanwise locations. There are variations in the temperature at different spanwise locations. The variation increases in Fig.20 (b) as the top and bottom span locations are further away from the center of the tunnel. Although the spanwise variations of the model surface temperature with other icing conditions are not shown here, the results showed very similar trends.

### Concluding Remarks

Tests to investigate the repeatability of the ice shape and resulting drag were performed, and the results were presented. This test program also provided a new database for code validation work. Several findings from the test include the following:

1. The repeatability of the ice shape was fair at near freezing temperatures, and the repeatability improved as the ice shape changed from glaze to rime ice. The repeatability of the ice shape was very good at  $-15^{\circ}\text{F}$ .
2. An increase in the airspeed did not affect the repeatability in the ice shape and drag.
3. The accretion time did not affect the repeatability of the ice shape.
4. The repeatability of the ice shape did not deteriorate with LWC.
5. Both standard and mod-1 nozzles gave the same results for a common icing condition.
6. All the major characteristics in the ice shape were preserved along the span within the uniform test section cloud. The quantity of ice accreted decreased with distance from the center of the tunnel for the mod-1 nozzles. For the standard nozzles, the quantity of ice accreted at the mid- and the bottom-span locations was very close, but less accretion of ice was seen at the top-span location.
7. The results from the surface temperature measurements showed that latent heat released from freezing droplets during ice accretion raised

the surface temperature as much as 17 degrees during the initial phase of the accretion.

More tests are planned to document the effects of other icing parameters on the repeatability of the ice shape and resulting drag. It is also planned to obtain experimental lift data with iced airfoils for code validation work.

### References

1. Soeder, R.H. and Andracchio, C.R., "NASA Lewis Icing Research Tunnel User Manual," NASA TM 102319, 1990.
2. Shaw, R.J., Sotos, R.G., "An Experimental Study of Airfoil Icing Characteristics," NASA TM 82790, 1982.
3. Olsen, W, Shaw, R., and Newton, J., "Ice Shapes and the Resulting Drag Increase for a NACA 0012 Airfoil," NASA TM 83556, 1984.
4. Abbott, I.H. and Von Doenhoff, A.E., Theory of Wing Sections, pp. 462-463, Dover Publications, Inc., 1959.
5. Blaha, B.J. and Evanich, P.L., "Pneumatic Boot for Helicopter Rotor Deicing," NASA CP-2170, 1980.
6. Gregory, N. and O'Reilly, C.L., "Low-Speed Aerodynamic Characteristics of NACA 0012 Airfoil Section, Including the Effects of Upper-Surface Roughness Simulating Hoar Frost," NPL AERO Report 1308, 1970.
7. Ide, R.F., "Liquid Water Content and Droplet Size Calibration of the NASA Lewis Icing Research Tunnel," NASA TM 102447, 1990.

**Table 1. Test Conditions for the Effects of Air Temperature and Accretion Time**

Model: NACA 0012 airfoil

Span: 6 ft.

Chord: 21 in.

Angle of Attack: 4°

Volume Median droplet Diameter: 20 µm

Air Speed (mph)	LWC (g/m <sup>3</sup> )	Total Temperature (°F)	Ice Accretion Time (min.)
150	1.0	28	6
150	1.0	25	6
150	1.0	22	6
150	1.0	18	6
150	1.0	12	6
150	1.0	1	6
150	1.0	-15	6
230	0.55	28	7
230	0.55	25	7
230	0.55	22	7
230	0.55	18	7
230	0.55	12	7
230	0.55	1	7
230	0.55	-15	7
150	1.0	28	12
150	1.0	25	12
150	1.0	22	12
150	1.0	18	12
150	1.0	12	12



Table 2. Test Conditions for the Effects of LWC

Model: NACA 0012 airfoil

Span: 6 ft.

Chord: 21 in.

Angle of Attack:  $4^\circ$

Volume Median droplet Diameter:  $30\ \mu\text{m}$

Air Speed (mph)	LWC ( $\text{g/m}^3$ )	Total Temperature ( $^\circ\text{F}$ )	Ice Accretion Time (min.)
230	1.0	22	6
230	1.3	22	6
230	1.6	22	6
230	1.8	22	6

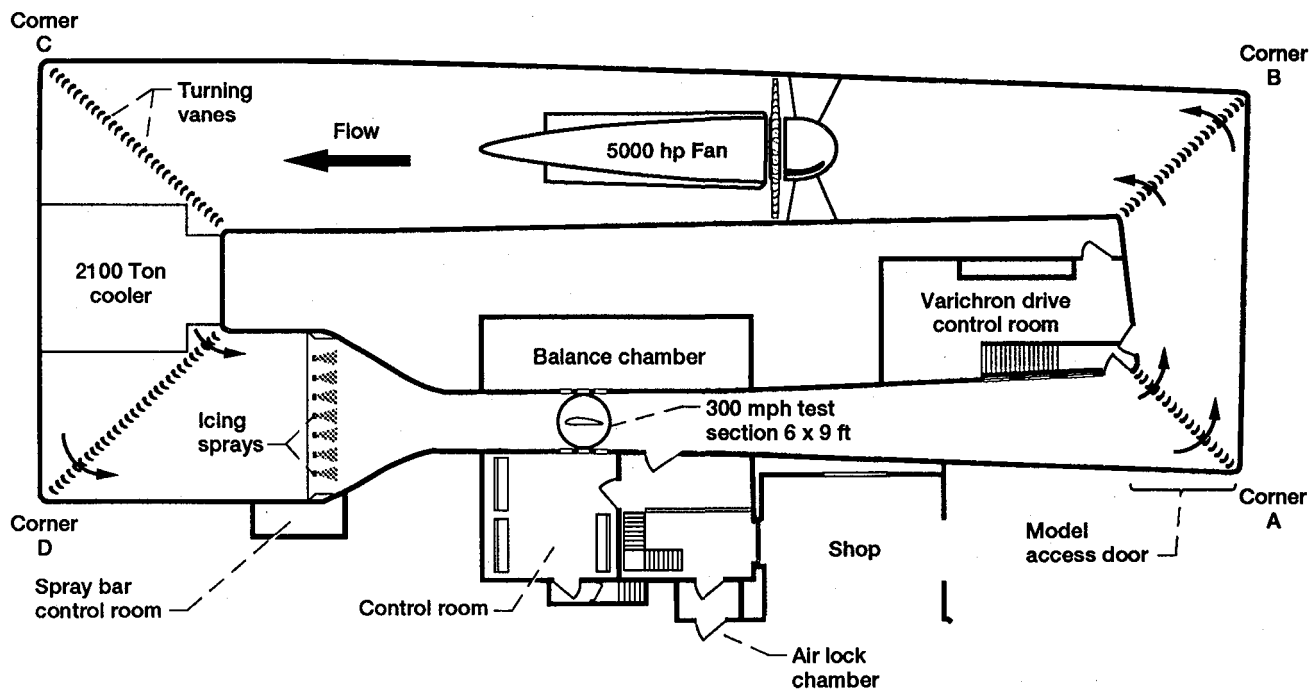


Figure 1.—Plan view of Icing Research Tunnel, shop, and control room.

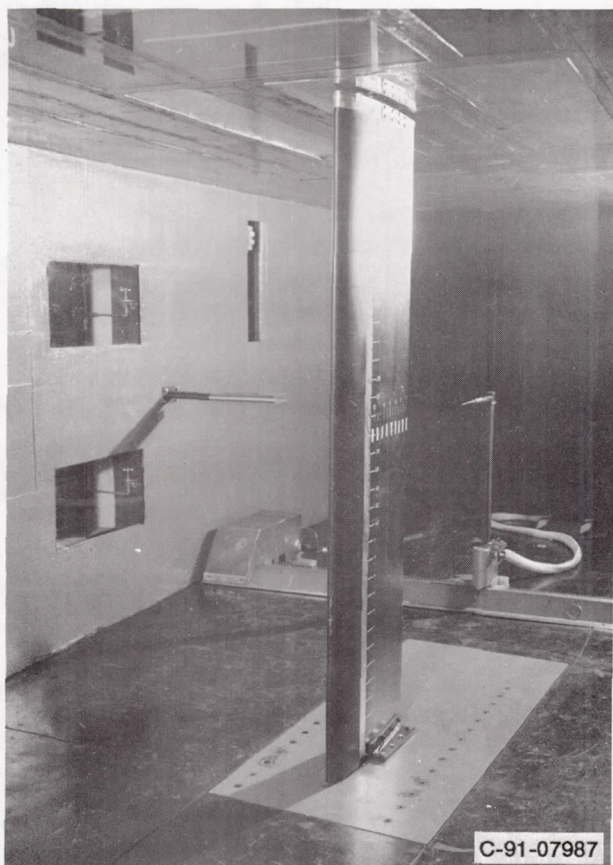


Figure 2.—NACA 0012 airfoil and wake survey probe.

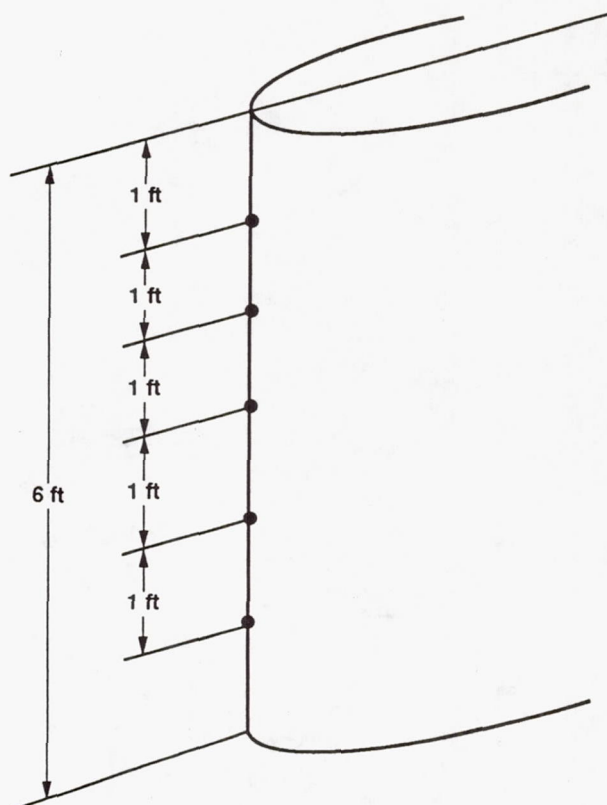


Figure 3.—Thermocouple locations on NACA 0012 airfoil.

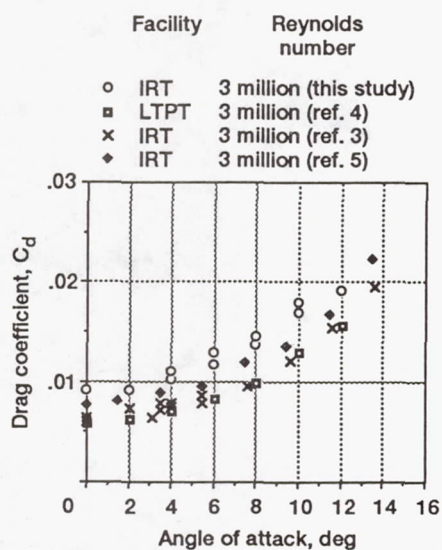


Figure 4.—Comparison of measured clean airfoil drag with published data for the NACA 0012 airfoil.

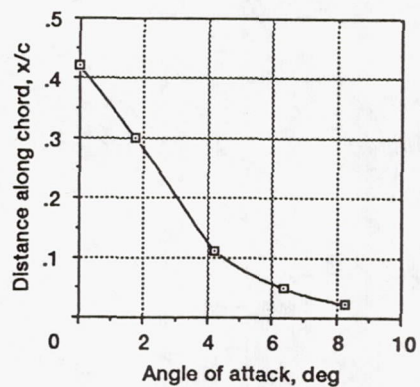


Figure 5.—Transition locations on the NACA 0012 airfoil for  $Re = 2.88 \times 10^6$ .

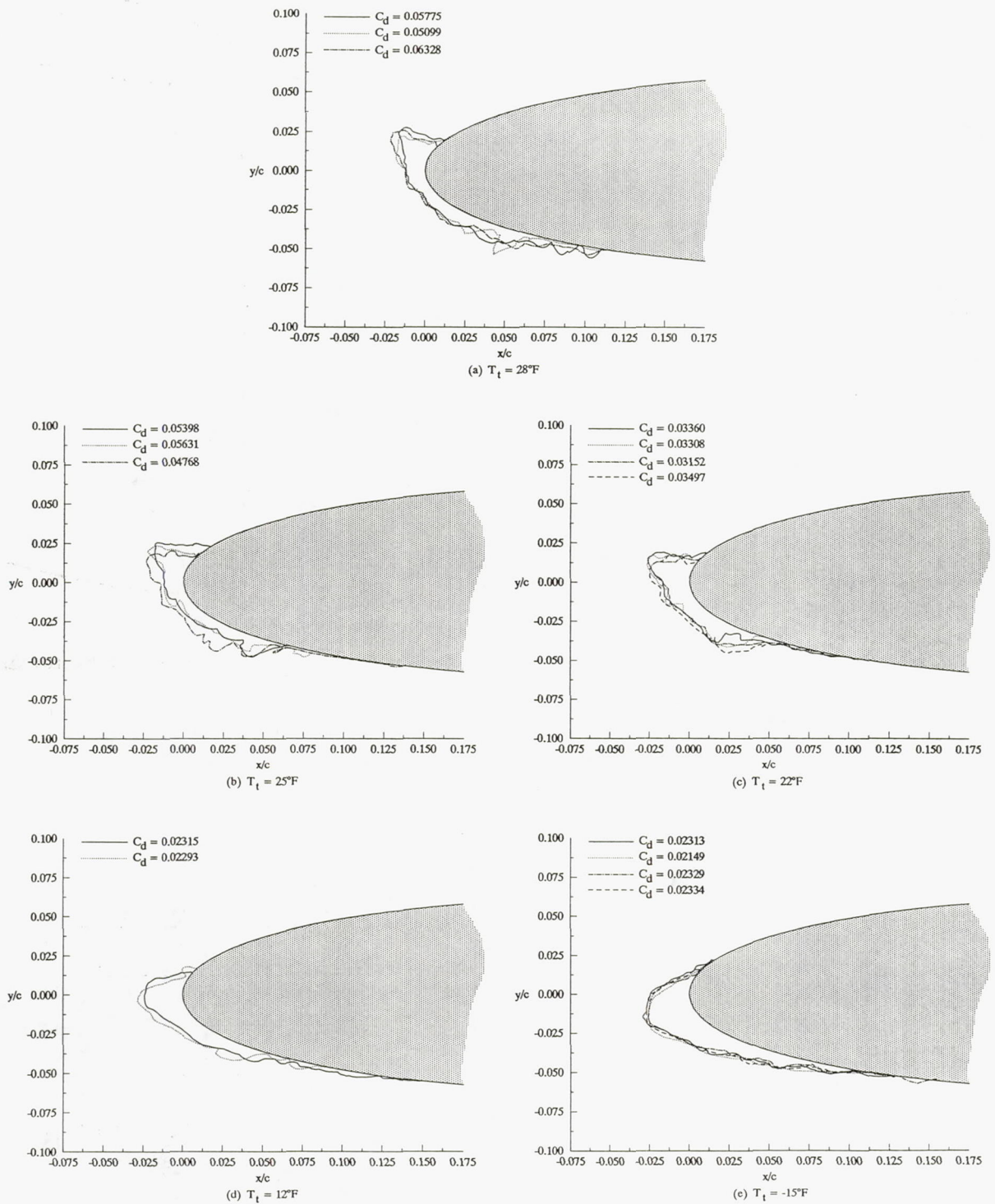


Figure 6.—Repeatability of ice shape and drag coefficient with total air temperature for  $\alpha = 4^\circ$ ,  $V_\infty = 150$  mph,  $\text{LWC} = 1.0 \text{ g/m}^3$ ,  $\text{MVD} = 20 \text{ }\mu\text{m}$ ,  $t = 6 \text{ min}$ .



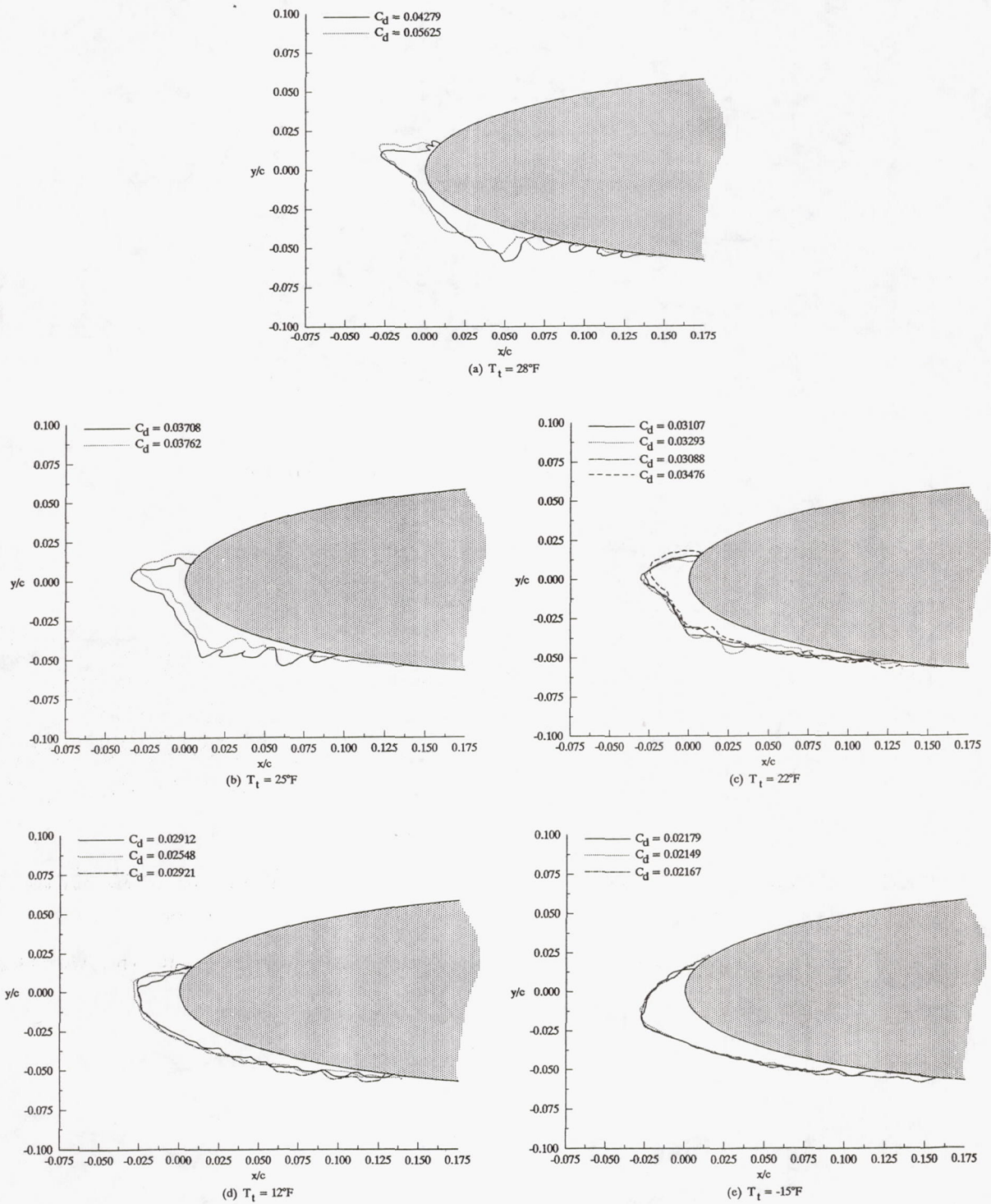


Figure 7.—Repeatability of ice shape and drag coefficient with total air temperature for  $\alpha = 4^\circ$ ,  $V_\infty = 230$  mph,  $LWC = 0.55$  g/m<sup>3</sup>,  $MVD = 20$   $\mu\text{m}$ ,  $t = 7$  min.

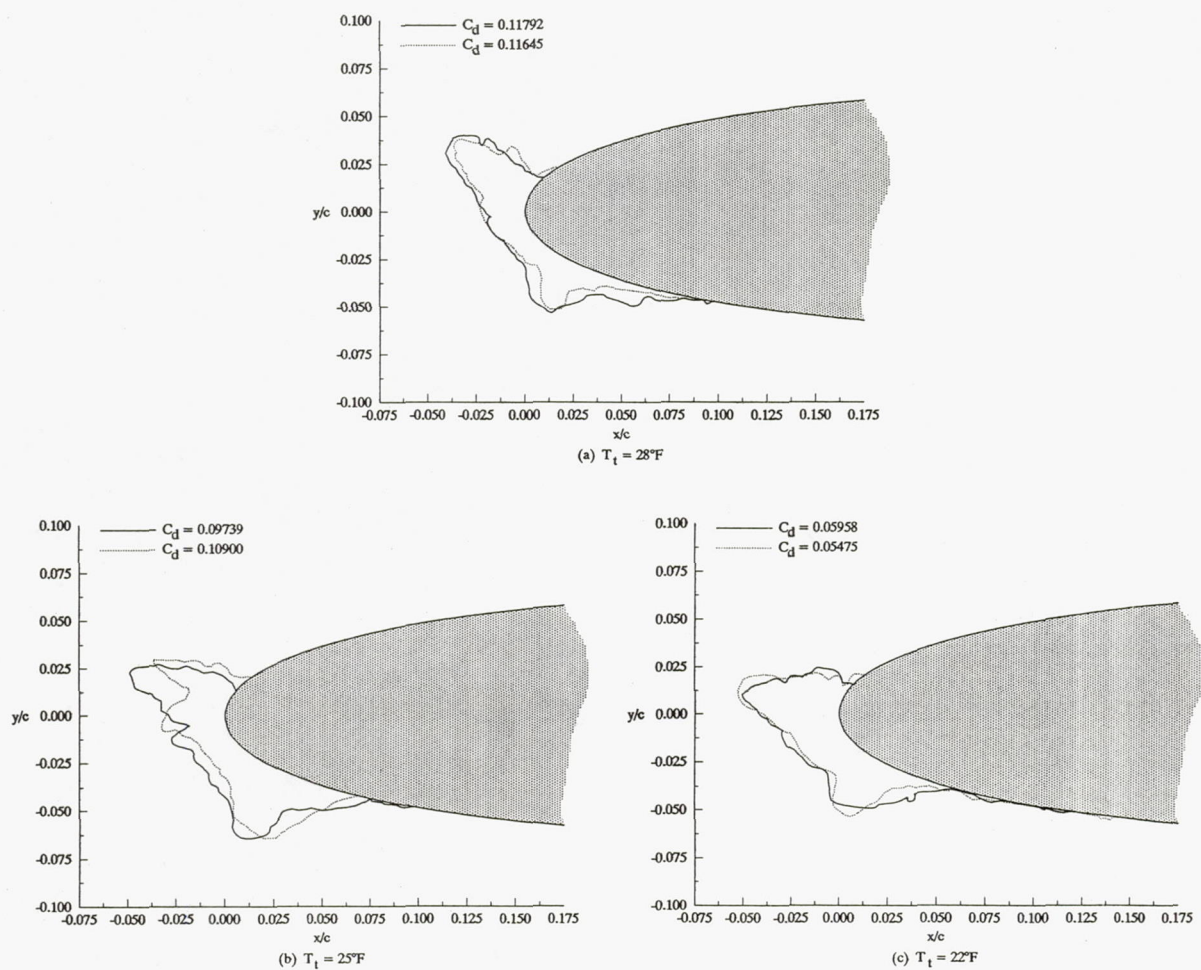


Figure 8.—Repeatability of ice shape and drag coefficient with total air temperature for  $\alpha = 4^\circ$ ,  $V_\infty = 150$  mph,  $\text{LWC} = 1.0 \text{ g/m}^3$ ,  $\text{MVD} = 20 \text{ }\mu\text{m}$ ,  $t = 12$  min.



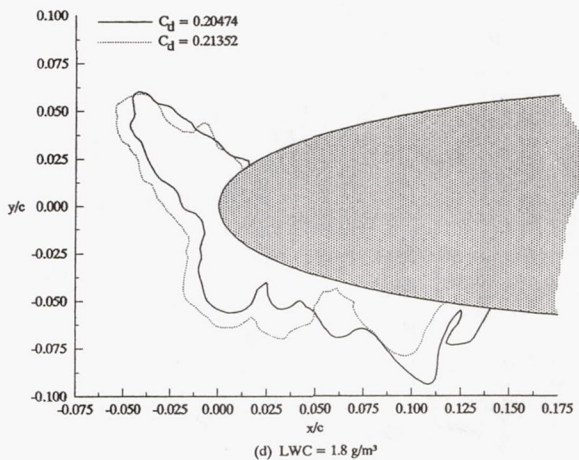
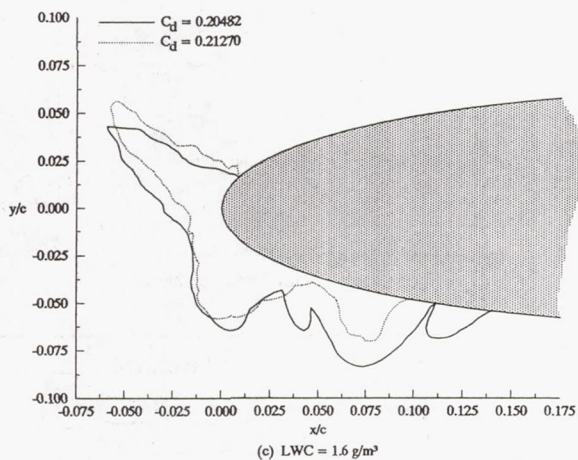
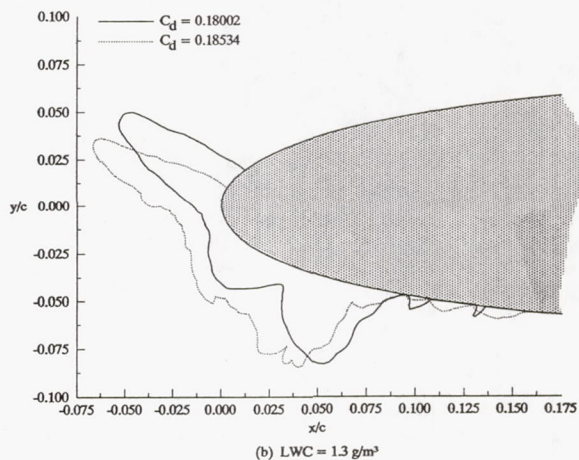
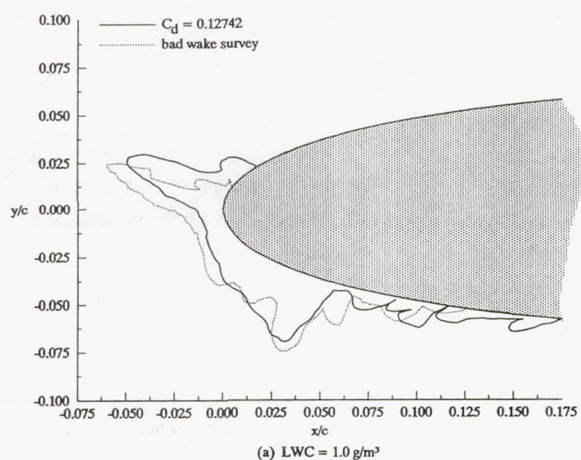


Figure 9.—Repeatability of ice shape and drag coefficient with liquid water content for  $\alpha = 4^\circ$ ,  $V_\infty = 230$  mph,  $T_t = 22^\circ\text{F}$ , MVD =  $30\ \mu\text{m}$ ,  $t = 6$  min.

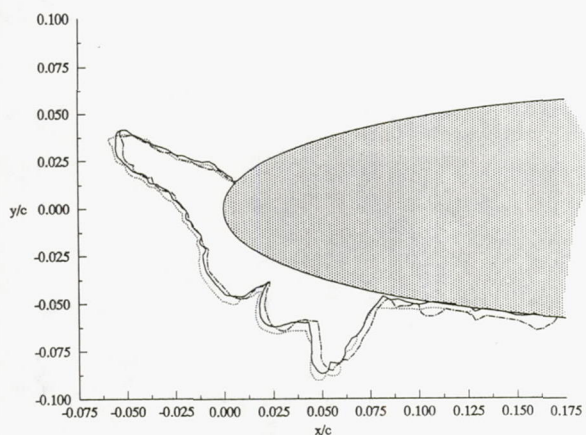


Figure 10.—Comparison of ice shape taken by three data takers ( $\alpha = 4^\circ$ ,  $V_\infty = 230$  mph,  $T_t = 22^\circ\text{F}$ ,  $\text{LWC} = 1.3 \text{ g/m}^3$ ,  $\text{MVD} = 30 \mu\text{m}$ ,  $t = 6$  min).

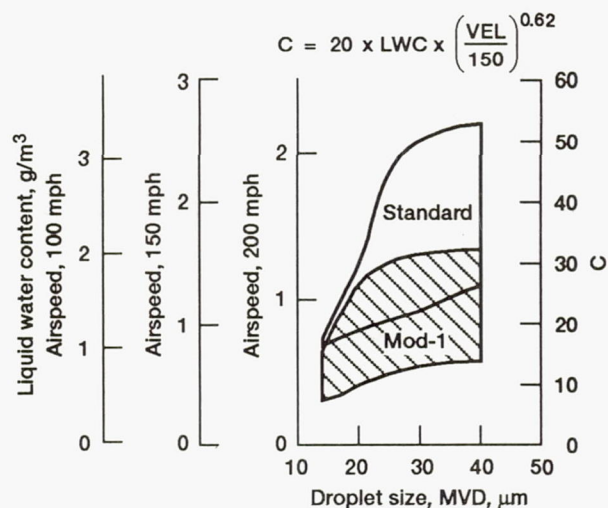


Figure 11.—NASA Lewis IRT operating envelopes.

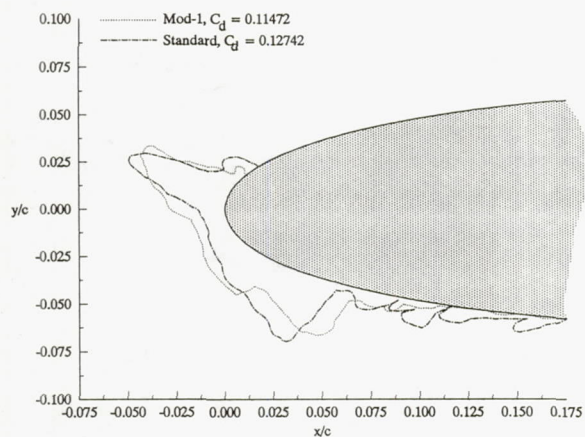


Figure 12.—Comparison of ice shape obtained from standard and Mod-1 nozzles for  $\alpha = 4^\circ$ ,  $V_\infty = 230$  mph,  $T_t = 22^\circ\text{F}$ ,  $\text{LWC} = 1.0 \text{ g/m}^3$ ,  $\text{MVD} = 30 \mu\text{m}$ ,  $t = 6$  min.

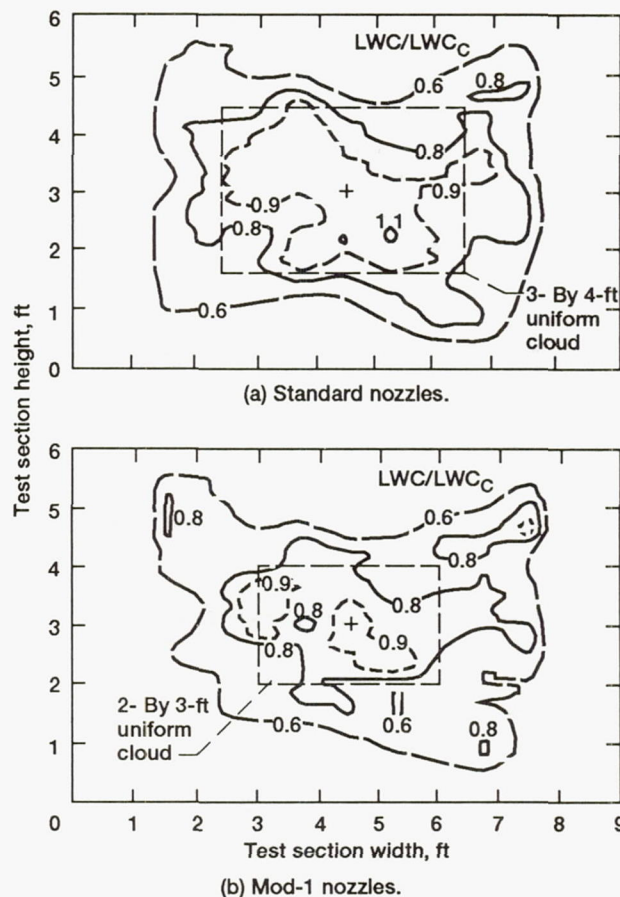


Figure 13.—Contour maps of liquid water content distribution in NASA Lewis IRT test section.

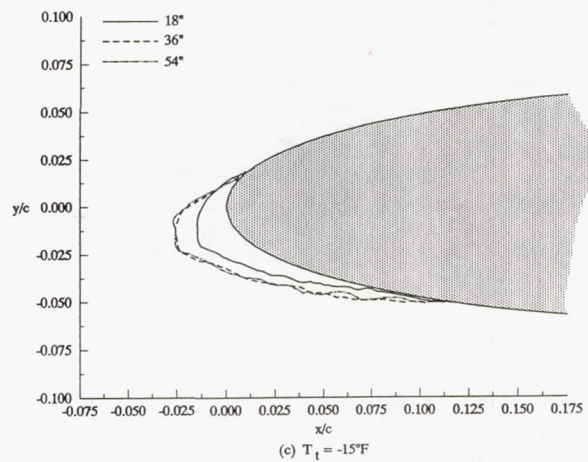
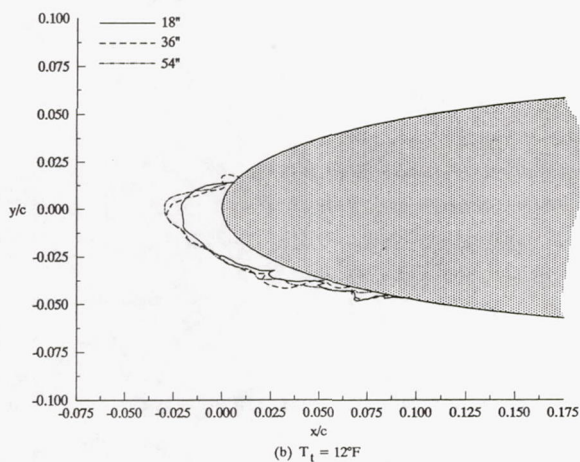
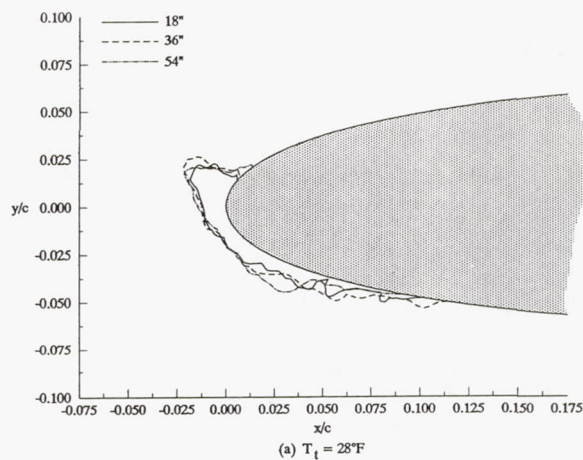


Figure 14.—Spanwise variation of ice shape with standard nozzles ( $\alpha = 4^\circ$ ,  $V_\infty = 150$  mph,  $\text{LWC} = 1.0 \text{ g/m}^3$ ,  $\text{MVD} = 20 \mu\text{m}$ ,  $t = 6$  min).



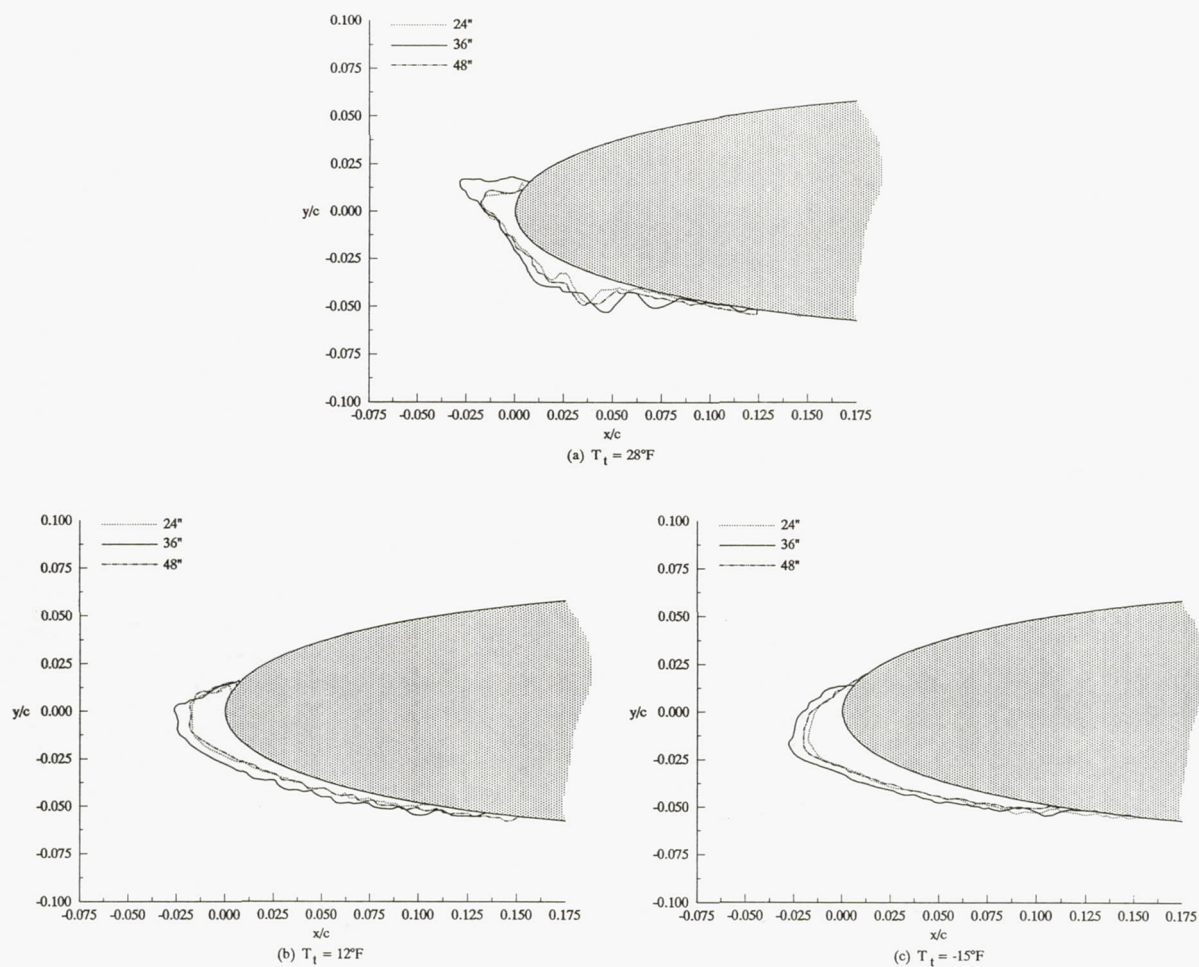


Figure 15.—Spanwise variation of ice shape with Mod-1 nozzles ( $\alpha = 4^\circ$ ,  $V_\infty = 230$  mph,  $\text{LWC} = 0.55 \text{ g/m}^3$ ,  $\text{MVD} = 20 \mu\text{m}$ ,  $t = 7$  min).

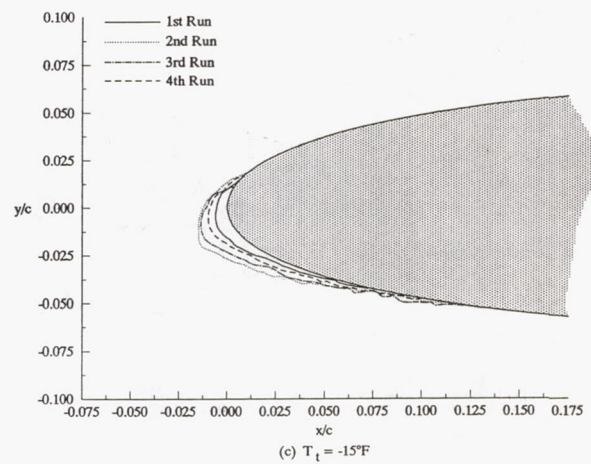
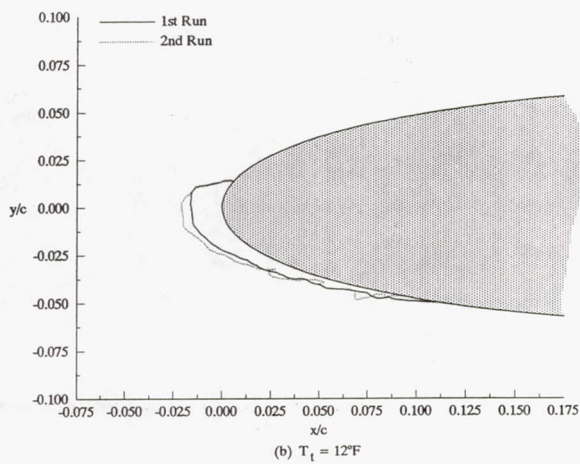
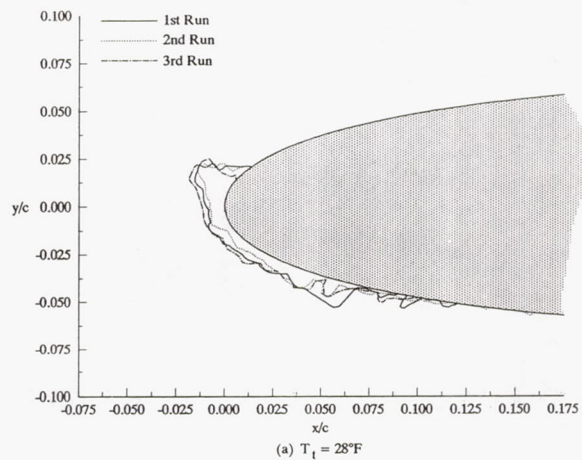


Figure 16.—Repeatability of ice shape at the top span location ( $\alpha = 4^\circ$ ,  $V_\infty = 150$  mph,  $\text{LWC} = 1.0 \text{ g/m}^3$ ,  $\text{MVD} = 20 \mu\text{m}$ ,  $t = 6$  min).



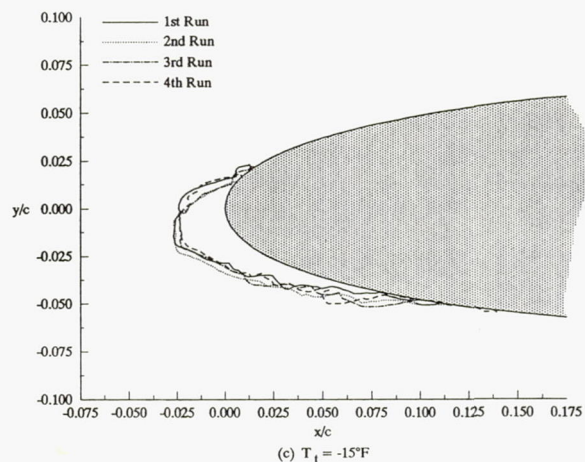
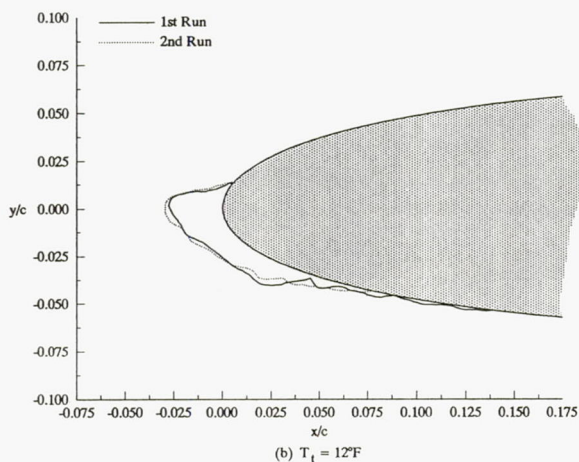
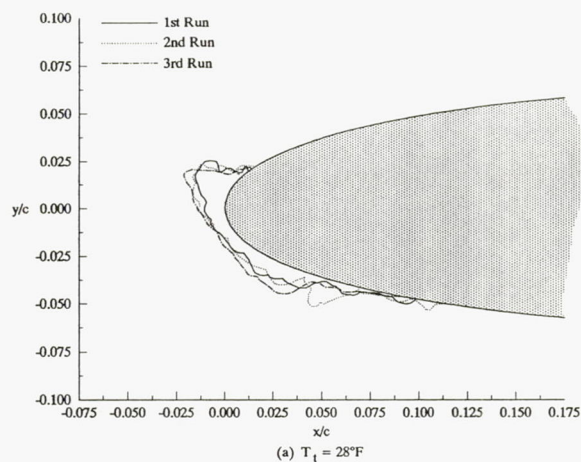


Figure 17.—Repeatability of ice shape at the bottom span location ( $\alpha = 4^\circ$ ,  $V_\infty = 150$  mph,  $\text{LWC} = 1.0 \text{ g/m}^3$ ,  $\text{MVD} = 20 \mu\text{m}$ ,  $t = 6$  min).

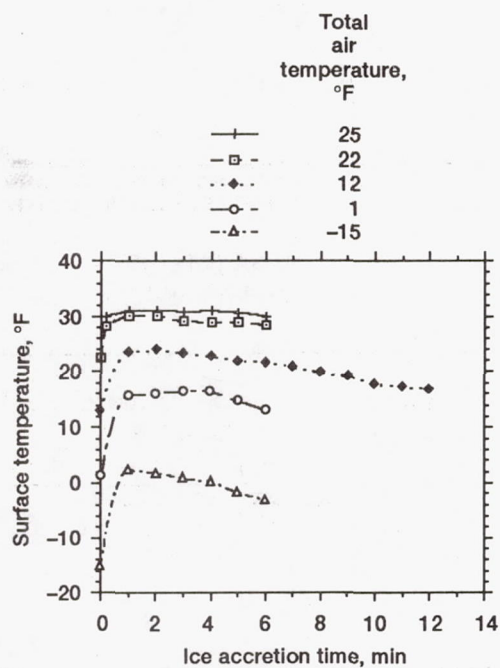


Figure 18.—Surface temperature histories of model leading edge at mid-span ( $\alpha = 4^\circ$ ,  $V_\infty = 150$  mph,  $LWC = 1.0 \text{ g/m}^3$ ,  $MVD = 20 \mu\text{m}$ ).

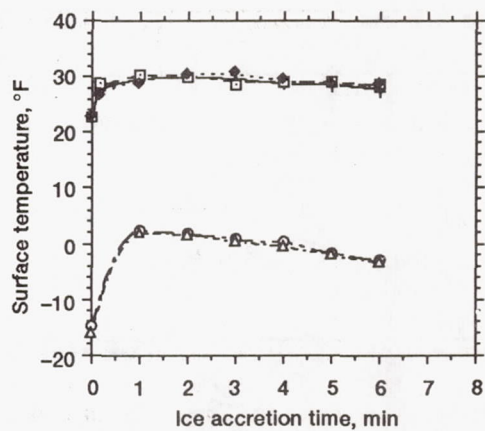


Figure 19.—Repeatability of model surface temperature of the leading edge at mid-span for total air temperatures of 22 and  $-15^\circ\text{F}$  ( $\alpha = 4^\circ$ ,  $V_\infty = 150$  mph,  $LWC = 1.0 \text{ g/m}^3$ ,  $MVD = 20 \mu\text{m}$ ).

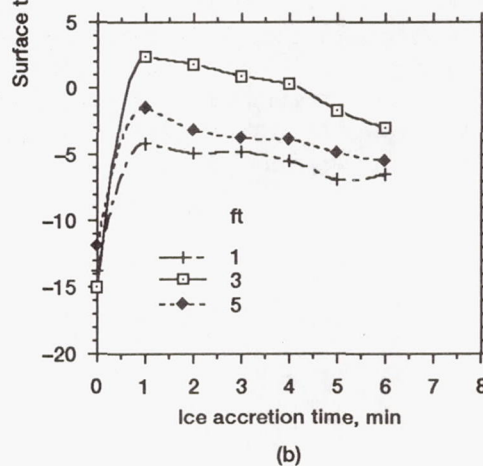
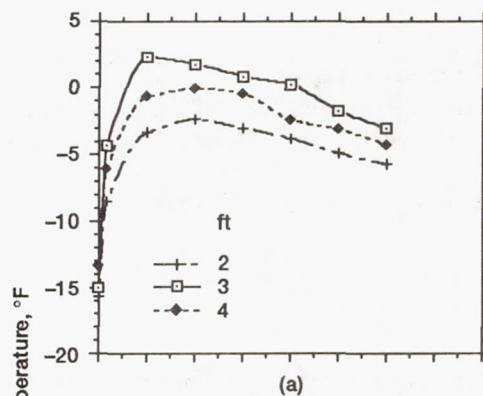


Figure 20.—Spanwise variation of model surface temperature at the leading edge ( $\alpha = 4^\circ$ ,  $V_\infty = 150$  mph,  $LWC = 1.0 \text{ g/m}^3$ ,  $MVD = 20 \mu\text{m}$ ).

**REPORT DOCUMENTATION PAGE**

Form Approved

OMB No. 0704-0188

Public reporting burden for this collection of information is estimated to average 1 hour per response, including the time for reviewing instructions, searching existing data sources, gathering and maintaining the data needed, and completing and reviewing the collection of information. Send comments regarding this burden estimate or any other aspect of this collection of information, including suggestions for reducing this burden, to Washington Headquarters Services, Directorate for Information Operations and Reports, 1215 Jefferson Davis Highway, Suite 1204, Arlington, VA 22202-4302, and to the Office of Management and Budget, Paperwork Reduction Project (0704-0188), Washington, DC 20503.

<b>1. AGENCY USE ONLY (Leave blank)</b>		<b>2. REPORT DATE</b> 1992	<b>3. REPORT TYPE AND DATES COVERED</b> Technical Memorandum	
<b>4. TITLE AND SUBTITLE</b> Results of an Icing Test on a NACA 0012 Airfoil in the NASA Lewis Icing Research Tunnel			<b>5. FUNDING NUMBERS</b>  WU-505-68-10	
<b>6. AUTHOR(S)</b> Jaiwon Shin and Thomas H. Bond				
<b>7. PERFORMING ORGANIZATION NAME(S) AND ADDRESS(ES)</b>  National Aeronautics and Space Administration Lewis Research Center Cleveland, Ohio 44135-3191			<b>8. PERFORMING ORGANIZATION REPORT NUMBER</b>  E-6761	
<b>9. SPONSORING/MONITORING AGENCY NAMES(S) AND ADDRESS(ES)</b>  National Aeronautics and Space Administration Washington, D.C. 20546-0001			<b>10. SPONSORING/MONITORING AGENCY REPORT NUMBER</b>  NASA TM-105374 AIAA-92-0647	
<b>11. SUPPLEMENTARY NOTES</b> Prepared for the 30th Aerospace Sciences Meeting and Exhibit sponsored by the American Institute of Aeronautics and Astronautics, Reno, Nevada, January 6-9, 1992. Responsible person, Jaiwon Shin, (216) 433-8714.				
<b>12a. DISTRIBUTION/AVAILABILITY STATEMENT</b>  Unclassified - Unlimited Subject Category 02			<b>12b. DISTRIBUTION CODE</b>	
<b>13. ABSTRACT (Maximum 200 words)</b>  Tests were conducted in the Icing Research Tunnel (IRT) at the NASA Lewis Research Center to document the current capability of the IRT, focused mainly on the repeatability of the ice shape over a range of icing conditions. Measurements of drag increase due to the ice accretion were also made to document the repeatability of drag. Surface temperatures of the model were obtained to show the effects of latent-heat release by the freezing droplets and heat transfer through the ice layer. The repeatability of the ice shape was very good at low temperatures, but only fair at near freezing temperatures. In general, drag data shows good repeatability.				
<b>14. SUBJECT TERMS</b> Ice accretion; Repeatability			<b>15. NUMBER OF PAGES</b> 20	
			<b>16. PRICE CODE</b> A03	
<b>17. SECURITY CLASSIFICATION OF REPORT</b> Unclassified	<b>18. SECURITY CLASSIFICATION OF THIS PAGE</b> Unclassified	<b>19. SECURITY CLASSIFICATION OF ABSTRACT</b> Unclassified	<b>20. LIMITATION OF ABSTRACT</b>	







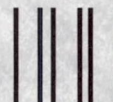
National Aeronautics and  
Space Administration

**Lewis Research Center**  
Cleveland, Ohio 44135

Official Business  
Penalty for Private Use \$300

**FOURTH CLASS MAIL**

ADDRESS CORRECTION REQUESTED



Postage and Fees Paid  
National Aeronautics and  
Space Administration  
NASA 451

**NASA**

---